The streamgauging ruler: A low-cost, low-tech, alternative discharge measurement technique

J. Le Coz, M. Lagouy, F. Pernot, A. Buffet, C. Berni

Journal of Hydrology 642 (2024) 131887

Contents lists available at ScienceDirect

Journal of Hydrology

journal homepage: www.elsevier.com/locate/jhydrol

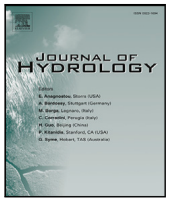

Research papers

The streamgauging ruler: A low-cost, low-tech, alternative discharge measurement technique

J. Le Coz *, M. Lagouy, F. Pernot, A. Buffet, C. Berni

INRAE, UR RiverLy, River Hydraulics, 5 rue de la Doua 69100 Villeurbanne, France

ARTICLE INFO

This manuscript was handled by Marco Borga, Editor-in-Chief, with the assistance of George Constantinescu, Associate Editor.

Keywords:
Velocity-head rod
Low-cost
Hydrometry
Streamgauging
Uncertainty

ABSTRACT

The streamgauging ruler, a.k.a. transparent velocity-head rod, is an inexpensive, easy, and quick tool for conducting wading discharge measurements in open-channel flows. It provides reliable velocity and discharge measurements when the right measuring conditions, especially minimum flow velocity, are met. The principle is simple: depth-averaged velocity can be computed from the water level difference between the upstream and downstream sides of a plastic board placed into the flow perpendicular to the flow direction. The model developed by INRAE (commercially available for €210) is a little more expensive than previously published models but it significantly improves the ease-of-use and measurement quality. Comparison experiments with reference measurements performed in a laboratory flume and at various field sites confirm the accuracy of the semi-empirical velocity rating established by Pike et al. (2016). Over most of the investigated cross-sections, the discharge measurements are generally within 10% of the reference discharge, when the velocity is greater than 0.2 m/s. However, operator-related effects (site selection, number and distribution of verticals, adjustment and reading of the sliding rulers) can lead to larger errors, hence operator training and care are essential.

A first evaluation of the velocity uncertainty related to the velocity-head reading is proposed in the form of an equation that can be used in existing methods for calculating discharge measurement uncertainty. As the method is extremely simple and quick, it is well suited for rapid discharge estimates, training or demonstration, citizen science programmes, or cooperation with services with limited resources and/or lacking specialized expertise in hydrometry. As of July 2024, 304 instruments had been built and released to diverse users around the world, along with a simple discharge computing spreadsheet, a video tutorial, and a field memo.

1. Introduction

Research, management, and decision making relating to water resources and water-related hazards are based on hydrological data, notably streamflow measurements and time series (McMillan et al., 2017). Most often, streamflow time series are derived from water level records using stage-discharge models (rating curves) which are established using streamgaugings, i.e. occasional measurements of stage and discharge. Streamgauging methods are diverse and generally require expensive and complex equipment, especially with the development of electronic instruments and discharge computation software. Volumetric or float streamgauging techniques are notable exceptions, however they are often difficult to implement correctly and limited to small discharges. As a result of cost and complexity, the spatio-temporal resolution of available hydrological data is often limited and observations are difficult to extend beyond institutional hydrometric networks (Strobl et al., 2020).

It is therefore useful to develop and validate alternative streamgauging systems that are inexpensive, easy to deploy and build, and sufficiently reliable and accurate for the intended purpose of the data. Alternative low-cost techniques may improve discharge measurements in specific site conditions and/or would be more affordable for training purposes and/or use in developing countries or remote regions. Innovative low-cost solutions are often revisited, modernized versions of old and sometimes forgotten instruments and techniques. For instance, Storz (2016) used solid steel spheres as hydraulic pendulums to measure floods in Ethiopia. This technique, used by Guglielmini (1690) and others before him, is a safe and inexpensive alternative to suspended current-meters in flood conditions. Also, floats historically used by Leonardo Da Vinci ca. 1500 (L'Hôte, 1990) and Mariotte in 1686 (Di Fidio and Gandolfi, 2011) have been used continuously, and now have their modern counterpart: surface velocity methods based on radar (Costa et al., 2006; Welber et al., 2016) or image

* Corresponding author.
E-mail addresses: jerome.lecoz@inrae.fr (J. Le Coz), mickael.lagouy@inrae.fr (M. Lagouy), francis.pernot@laposte.net (F. Pernot), alexis.buffet@inrae.fr (A. Buffet), celine.berni@inrae.fr (C. Berni).

https://doi.org/10.1016/j.jhydrol.2024.131887
Received 20 March 2024; Received in revised form 12 July 2024; Accepted 18 August 2024
Available online 23 August 2024

velocimetry (Fujita et al., 1998; Muste et al., 2008), the latter requiring relatively cheap equipment. These surface velocity streamgauging techniques can be applied safely in flood conditions. However, they can be affected by substantial sources of uncertainty (Le Coz et al., 2021), especially due to bed scour or fill, and estimation of the depth-averaged velocity to surface velocity ratio (Biggs et al., 2023). The rising bubble technique (Hilgersom and Luxemburg, 2012; Wilding et al., 2016) is another innovative, low-cost and low-tech method for accurate velocity measurements in slow and possibly weedy streams, making it useful for low flow conditions and water resources management, mainly. This technique relates to the rising body method developed by Bureau (1910) as early as in the beginning of the 20th century, measuring the trajectory of an empty iron sphere released from the bottom of a clear-water canal.

Among alternative low-cost streamgauging techniques, the transparent velocity-head rod, which we rename as streamgauging ruler for simplicity, was introduced by Fonstad et al. (2005) and improved by Pike et al. (2016) based on earlier models. It appears as a cost-efficient solution for wading streamgauging. Since the velocity-head rod described by Wilm and Storey (1944), a simple beveled and graduated wooden board (Fig. 1 a and b), was first introduced, the measurement principle has remained the same. The water level difference Δh (in meters) between upstream and downstream of the board oriented perpendicular to the flow direction increases with the dynamic head related to the depth-averaged flow velocity V (in m/s). Indeed, as the flow is stopped by the obstacle, its kinetic energy is transformed into potential energy. The same board oriented parallel to the flow direction can be used to measure the flow depth. The usual velocity-area streamgauging procedure (ISO748:2009, 2009) for currentmeters on wading rods can be applied to determine the discharge. At that time, the theoretical equality between kinetic energy and potential energy (Bernoulli principle) was used to determine the flow velocity:

$$V = \sqrt{2g\Delta h} \tag{1}$$

with $g = 9.81$ m/s^2 the gravity acceleration.

This measuring instrument has remained very marginal in hydrometry and forgotten even though some scientists sporadically used and developed the method. For example, Drost (1963) proposed a smaller version in metal (Fig. 1 c); Heede (1974) advised against the use of velocity-head rods in boulder-strewn mountain streams based on comparisons with currentmeter measurements and a San Dimas gauging flume; and Carufel (1980) provided a primer on the "construction and use of a velocity-head rod for measuring stream velocity and flow". More recently, Fonstad et al. (2005) introduced an inexpensive model in transparent plastic, fitted with sliding rulers. A significant advantage of a transparent instrument is that the operator no longer has to bend over and get closer to determine the water level on the upstream side of the instrument. Reading being done out of water once the rulers are positioned, substantial reading errors due to parallax are eliminated. Additionally, Fonstad et al. (2005) showed that a correction of Eq. (1) was necessary and they proposed the following empirical velocity rating:

$$V = 0.728\sqrt{2g\Delta h} - 0.1126 \tag{2}$$

This transparent velocity-head rod (Fig. 1 d) was further improved by Pike et al. (2016) to make it more robust and easier to build with the least expensive elements possible, and to improve the velocity rating. The main element is always a simple board of transparent plastic with dimensions 9.85 cm ×100 cm ×1.5 cm, the rulers being riveted or held by O-rings stretched with a door wedge. Based on 2400 velocity comparisons using an ADV SonTek FlowTracker as a reference (1-point measurements at 60% of the depth below the water surface) at 14 sites with 7 different operators, Pike et al. (2016) obtained the following velocity rating ($R^2 = 0.93$), slightly different from the previous one (Eq. (2)):

$$V = 0.641\sqrt{2g\Delta h} - 0.019 \tag{3}$$

Applying this velocity rating equation (Eq. (3)), the discharge root-mean square error (RMSE) computed by Pike et al. (2016) from their comparison tests was 10%.

King et al. (2022) used a different design, a 90° plastic 2.86×2.86 cm (0.1 × 0.1 ft) corner guard (Trimaco®), and a different velocity rating equation calibrated in a laboratory flume (Hundt and Blasch, 2019). While the discharge RMSE (10%) and mean error (−4%) in laboratory conditions (Hundt and Blasch, 2019) were as good as those reported by Pike et al. (2016), they were poorer in field conditions (King et al., 2022): median absolute error and median bias were 19.6% and +6.3%, respectively. Davids et al. (2019) used a flat plate 1 m-long by 34 mm-wide by 1.5 mm-thick and the raw velocity rating derived from the Bernoulli principle (Eq. (1)). From field measurements in Nepal conducted by themselves, experts, and citizen scientists, respectively, they obtained very poor performance indicators: mean absolute errors were 37%, 43%, and 131%, respectively, and mean biases were 26%, 40%, and 127%, respectively. Davids et al. (2019) and King et al. (2022) concluded that other streamgauging techniques like surface floats, rising body or salt dilution were more efficient for their needs. As stated by King et al. (2022), however, the uncertainty of the velocity and discharge results is very sensitive to the quality of the design and operation of the velocity-head rod, as well as the accuracy of its velocity rating. This is a motivation for further research and development on the improvement and uncertainty analysis of such a cost-efficient streamgauging technique.

In this paper, we report on the developments and tests that we have carried out since 2017 to validate and improve the velocity-head rod technique, through a model we call the streamgauging ruler. Some design improvements and technical solutions to practical problems (ease of use, field procedure, discharge computations, training materials) are presented in Section 2. Comparative field and laboratory tests were conducted to evaluate velocity and discharge errors (Section 3), and an estimation of velocity and flow measurement uncertainty is proposed (Section 4). Finally, prospects for the improvement and dissemination of the technique, as well as some thoughts on why the experimental velocity rating deviates from theory are discussed (Section 5).

2. Improvement and operation of the streamgauging ruler

2.1. Instrument design and production

Since 2017, we have tested and incorporated several practical improvements to the prototype described by Pike et al. (2016) in order to facilitate and improve the measurement, while keeping the manufacturing cost around € 100 (the cost of mechanical, electromagnetic or acoustic Doppler currentmeters may be 10 to 100 times more).

First of all, the two commercially available rulers are replaced by an inexpensive plastic slider (red PMMA, 1.6 × 30 × 1000 mm) and an original model of engraved ruler (transparent thermoplastic PMMA, 2 × 60 × 1000 mm). The slider and the ruler are positioned upstream and downstream of the main board (transparent thermoplastic PMMA, 8×98.5×1000 mm), respectively. While the slider is narrow and opaque, the broader ruler is transparent and graduated in both height and velocity (cf. Fig. 2a), according to the velocity rating (Eq. (3)). This provides a direct determination of the flow velocity, which is usually appreciated by users even though only Δh is written in the field notes.

The slider and the ruler are fixed by neodymium iron boron magnets (diameter 12 mm, thickness 8 mm) inserted in the board that stick to 0.55 mm-thick, ferrous PVC rubber tapes glued to the rulers. This ensures a better adhesion and durability than O-rings or rubber bands which are often worn out or cut after some time. The slider and the ruler are held by plastic clips that are 3D printed (cf. Fig. 2e). The operator can make them slide easily along the board axis to adjust their positions to have them touching the water surface. Small holes at the top of the slider and the ruler (cf. Fig. 2h) are help to grasp them.

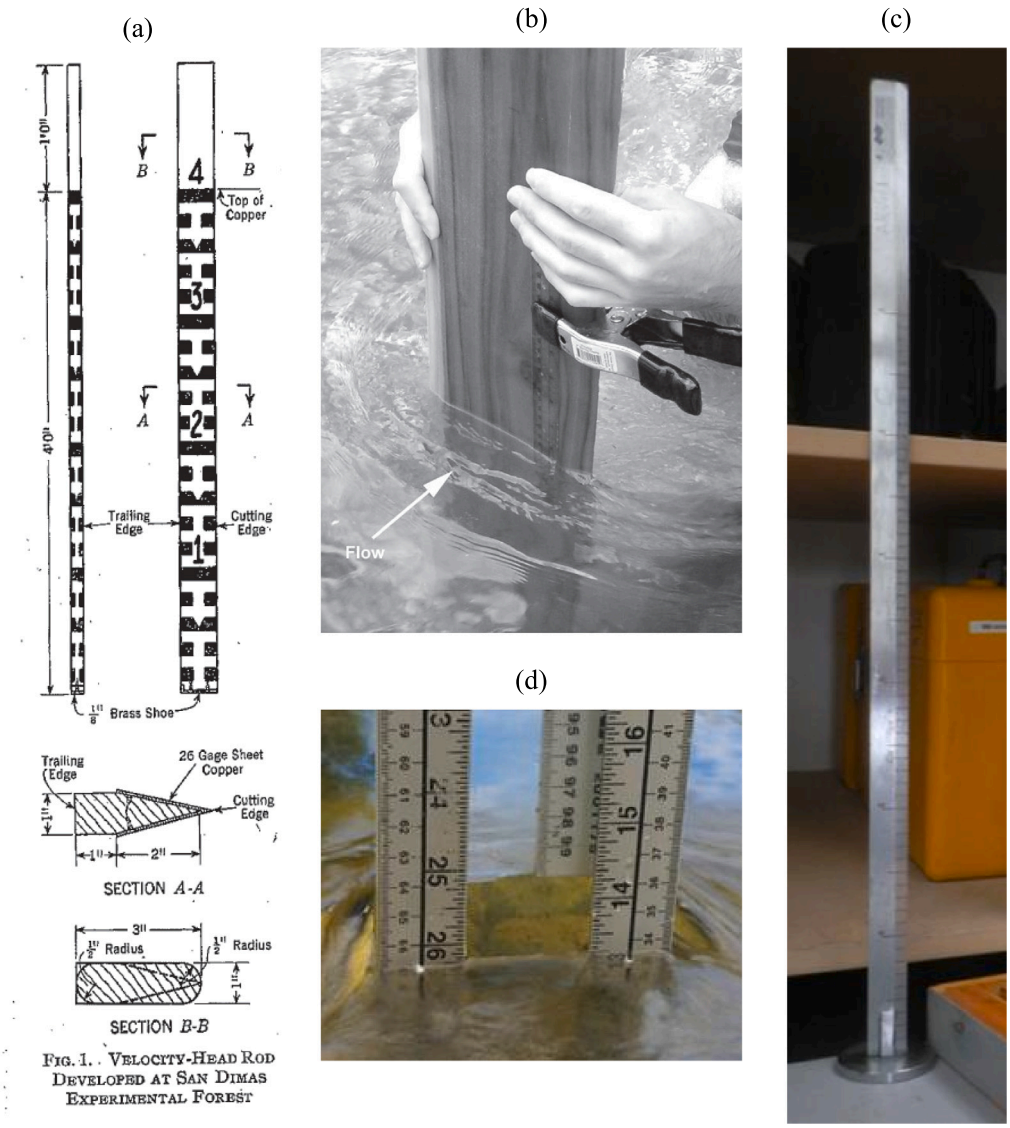

Fig. 1. Published velocity-head rod models: (a) wooden model of Wilm and Storey (1944) (b) reconstructed by Fonstad et al. (2005), (c) stainless steel model of Drost (1963) stored in a NIWA field measurement office in New Zealand (photo: J. Le Coz), (d) transparent model introduced by Fonstad et al. (2005) and modified by Pike et al. (2016).

A small spirit level (cf. Fig. 2d) helps the operator keep the board vertical. Graduations every half centimeter on one edge of the main plastic board (cf. Fig. 2d) make the flow depth easier and safer to measure than using the ruler, which otherwise would have to be aligned precisely with the bottom end of the board for depth measurements. In the most recent version (2022), the upper top of the slider has been graduated in millimeters so that Δh can be read here as well, since the ruler and the slider have exactly the same length (cf. Fig. 2h). Actually, this evolution was suggested by a student during a practical class in the field. A small 3D-printed cap keeps the right separation distance between slider and ruler and makes the reading easier.

The design files of the slider, ruler and main board (for 100 cm- and 60 cm-long boards), and the .stl files for 3D printing of the 4 clips and the cap are provided as supplementary materials. Clearly, this model of transparent velocity-head rod is slightly more difficult to build than others with usual tools. While the required pieces and materials are easily available, the equipment required for 3D-printing and precise plastic cutting and engraving is not accessible to all, hence outsourcing these production steps may be necessary. Since 2022, the INRAE model of streamgauging ruler has been commercially available from an independent French small business, AAIS,[1] for approximately € 210 VAT, shipping fees included. The authors and INRAE have no financial agreement with AAIS.

2.2. Field measurement procedure

The usual velocity-area streamgauging procedure (ISO748:2009, 2009) applies to streamgauging ruler discharge measurements. Good practices for velocity-area streamgauging are also crucial to the quality of streamgauging ruler discharge results, in particular the measurement site selection (and cleaning, if necessary), water level monitoring, number and distribution of verticals, and calculation of flow by interpolation and extrapolation to the edges. Compared to a wading streamgauging using a currentmeter mounted on a rod, the only specificities are the depth and velocity measurement related to the instrument itself. The procedure and main tips and limitations to keep in mind are summarized in a field memo in French and translated in English (cf. Fig. 3a) associated with the OFB-INRAE streamgauging manual (Le Coz et al.,

[1] AAIS - Atelier d'Art et d'Impression Sérigraphique - 9 Avenue des Buissières, 38360 Sassenage - France.

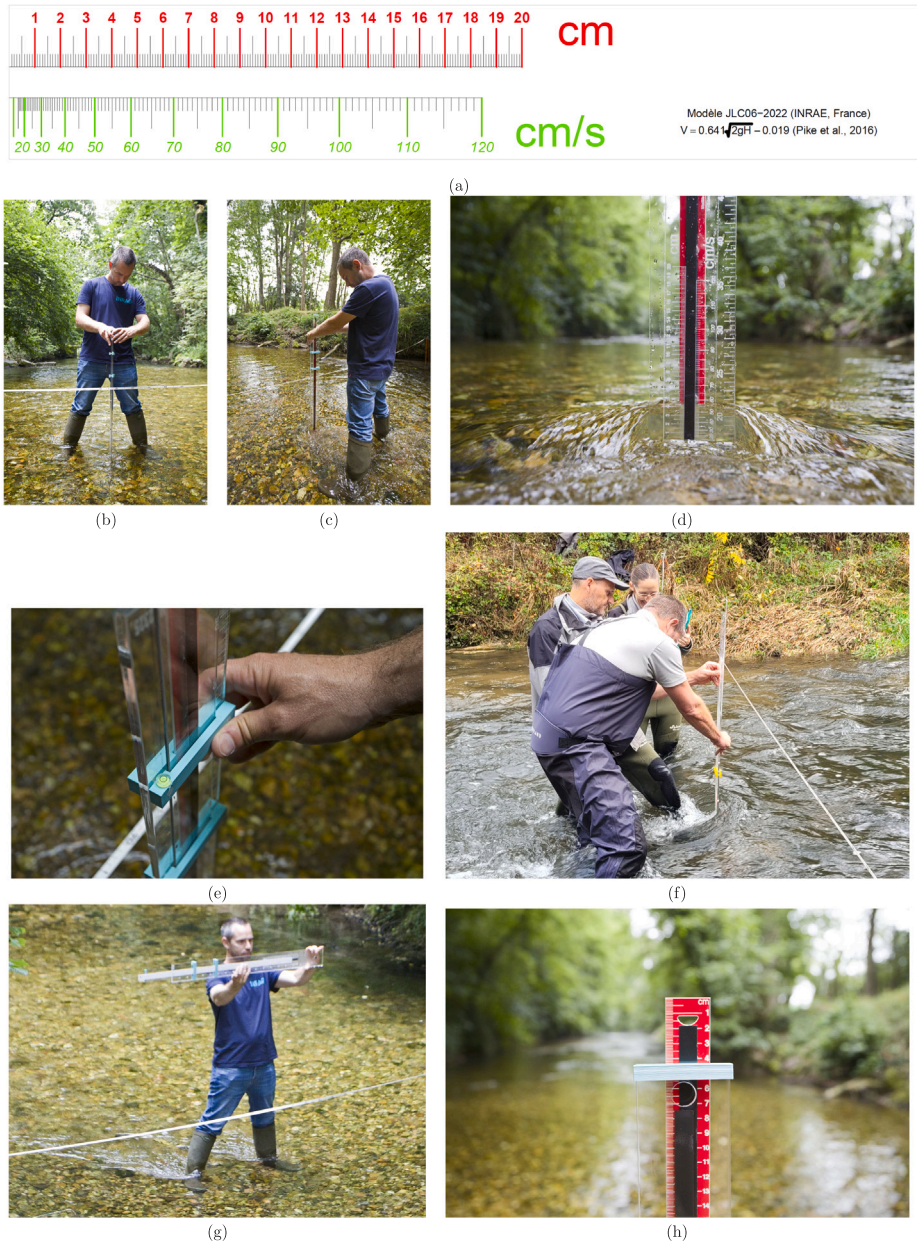

Fig. 2. Design and deployment of the streamgauging ruler, displaying the INRAE 2022 model: (a) design of the ruler graduated in velocity-head and velocity, using Eq. (3), (b) measuring the position across the river and the flow depth, (c) opposing the flat side of the board to the flow, (d) adjusting the (transparent) ruler and (red) slider at the water surface, (e) keeping the board vertical thanks to the spirit level, (f) avoiding flow disturbance unlike this counterexample of high-velocity measurements during a training session, reading the velocity-head (g) at the bottom of the board on the graduated ruler or (h) at the top of the board on the graduated slider. Photos courtesy of Rodolphe De Santis (b–e,g–h) and Guillaume Dramais (f).

2011). A user's guide for the "stream velocity board" (i.e. the velocity-head rod developed by Pike et al. (2016)) with similar information has been released in English and French by the British Columbia Ministry of Environment (https://a100.gov.bc.ca/pub/acat/documents/r50525/SVB_Guide_Eng_2021_1632844892300_C54252B9EC.pdf). We have also released a video tutorial (in English and French) on the Groupe Doppler Hydrométrie YouTube channel (https://youtu.be/Mv2mHpCYPos).

The recommended conditions of use are depths ranging from 2 to 70 cm (limit of graduations and operator holding in the flow) and velocities greater than 20 cm/s over most of the cross-section (or $\Delta h \geq$ 6 mm) and less than 1.2 m/s (limit of graduations and operator holding in the flow, water surface fluctuations). In practice, the lower velocity limit (20 cm/s) is the most limiting measurement condition.

The operator should stand downstream of the board legs apart, in order to minimize flow disturbance (cf. Fig. 2bc). On each measurement vertical, the operator reads and records three values: the abscissa (in m, usually) read on the ruler tape stretched across the watercourse, the flow depth (in cm, usually) and the water level difference Δh (in mm, usually). At the flow edges, only the abscissa and the flow depth are recorded.

The operator measures the depth with the board aligned with the flow (cf. Fig. 2b), in order to minimize flow disturbance, and kept vertical using the spirit level. The operator must keep in mind that flow depth measurements are used to compute the flow area around each vertical. Due to the width of the streamgauging ruler, it may be difficult to set the board at a representative bed elevation when the bed material is coarse, with possible underestimation of the mean flow depth. When the stream bed is soft and/or erodible, the board may sink and the flow depth may be overestimated (as might be the case when using a usual current meter rod as well). The water level can be read

either directly on the board in the water or by adjusting the ruler or the slider to the water surface, then removing the board from the water to read the graduations. In the first case, the edge of the board bearing the graduations are placed downstream to limit the impact of the bow wave created upstream of the board.

To measure the velocity, the board is oriented perpendicular to the flow, the slider without graduation upstream and the graduated ruler downstream, towards the operator (cf. Fig. 2c). Then, the bottom end of the ruler is adjusted to the downstream water level and the bottom end of the slider is adjusted to the upstream water level (cf. Fig. 2d). The adjustment must be done carefully, especially when the velocity hence Δh are small. For higher velocities, the free-surface elevation may fluctuate (especially upstream), in which case an average position of the ruler and slider should be determined. Pike et al. (2016) recommend averaging over 40 seconds (likely based on the ISO748:2009 (2009) standard recommendation for the time of exposure of currentmeters), however a shorter period is often sufficient in practice.

To apply the velocity rating, the flow must be free around each edge of the board. In practice, this implies that the lateral distance between the edge of the board and the channel edge or any other obstacle is not less than about 15 cm. It is also important that the flow passing under the toe of the board is minimal, even when the bed is uneven: the flow must be blocked by the board over the full depth. The streamgauging ruler should be kept vertical using the spirit level (cf. Fig. 2e), and flow disturbance by the operators should be minimized, especially for high flow velocities (cf. Fig. 2f: there are too many operators with their legs too close to the board). Very importantly, the velocity rating will be inaccurate for oblique flows. Unlike currentmeters or other velocimeters which can measure the velocity projection along their axis, the streamgauging ruler, being opposed perpendicularly to the direction of the flow, can only measure the velocity magnitude. Therefore, discharge should be measured at sites where the flow is reasonably perpendicular to the cross-section (i.e. to the tagline) over the full width. Otherwise, the angle between the board (or the flow) and the cross-section should be measured and used to calculate the velocity component normal to the cross-section, hence the discharge.

To avoid substantial parallax errors, Δh must not be read while the streamgauging ruler stands in the water (Pike et al., 2016). Instead, the instrument must be removed from the water and held horizontal and perpendicular to the gaze of the operator, arms outstretched in case of doubt (cf. Fig. 2g). The operator then reads precisely (at least to the nearest mm) the difference Δh in water levels and optionally the corresponding velocity. Alternatively, Δh can be read on the slider at the top of the board (cf. Fig. 2h) with two advantages: the instrument remains in the water (time and effort saved) and parallax error can be avoided.

2.3. Discharge computation

At each measurement position (or vertical) i ($1 \le i \le m$), the position x_i across the transect, the flow depth D_i and the velocity-head Δh_i are noted. The depth-averaged velocity V_i is computed from Δh_i using Eq. (3). At the channel edges ($i = 0$ or $i = m+1$), only the position and the flow depth are noted, the velocity being extrapolated using an edge coefficient C_i. Discharge Q is computed according to the conventional mid-section procedure (ISO748:2009, 2009):

$$Q = \sum_{i=0}^{m+1} B_i \; D_i \; V_i \tag{4}$$

where m is the number of verticals, indices $i = 0$ and $i = m + 1$ stand for edges, and B_i are the widths of the rectangular panels: $B_i = |x_{i+1} - x_{i-1}|/2$ for $1 \le i \le m$, $B_0 = |x_1 - x_0|/2$ and $B_{m+1} = |x_{m+1} - x_m|/2$. To extrapolate velocity from the nearest measurement to the edge, a power profile with exponent $1/C_i - 1$ is assumed. To get the right discharge integration using Eq. (4), we compute $V_0 = (2C_0 - 1)V_1$ and $V_{m+1} = (2C_{m+1} - 1)V_m$. Typical values of the edge coefficient are proposed, similar to the bottom coefficients proposed by the ISO748 standard (ISO748:2009, 2009) and to the edge coefficients used in ADCP software: 0.67 (sloped, natural edge), 0.91 (smooth, concrete vertical wall), 0.86 (intermediate situations). The edge coefficients can also be adjusted visually based on the measured velocity cross-profile.

This mid-section discharge computation has been implemented in a simple spreadsheet that can be used with Excel or LibreOffice (the current version is provided as supplementary material). Of course, discharge computation can be done with any conventional software used for velocity-area discharge measurement, provided that velocity-head values can be converted to velocity values. The left-hand area of the spreadsheet (cf. Fig. 3b) displays as field notes for entering the data and metadata of the streamgauging ruler discharge measurement. It may be printed to create paper field notes. Results are computed and displayed in the right-hand of the spreadsheet (cf. Fig. 3c) in the form of a results summary, a plot of depth and velocity cross-profiles, and uncertainty budget pie charts (not shown here).

On the velocity cross-profile, the ratio of each partial discharge $Q_i = B_i \; D_i \; V_i$ to the total discharge Q is displayed in green if smaller than 10%, in orange if it is between 10% and 15%, and in red beyond. The ISO748 standard (ISO748:2009, 2009) recommends that: "As far as possible, verticals should be chosen so that the discharge of each segment is less than 5% of the total and shall not exceed 10% of the total". However, this rule may impose measuring at too many verticals with no substantial gain in uncertainty if the depths, velocities and discharges are smoothly distributed along the cross-section. A better assessment is to quantify the discharge uncertainty resulting from the limited sampling of the lateral variability of the cross-section and flow, as proposed by methods like IVE, Q+ and Flaure (Despax et al., 2016). Uncertainty analysis will be introduced later in this paper.

3. Results of laboratory and field comparison tests

3.1. Velocity rating

To evaluate the velocity rating proposed by Pike et al. (2016), and to assess the measurement uncertainties and the limits of use, we carried out systematic comparisons of depth, depth-averaged velocity and discharge in the HHLab hydraulic laboratory of INRAE in Lyon and at various field sites in French rivers. The field measurements were conducted by INRAE and several regional offices (DREAL Grand-Est, Occitanie, Pays-de-Loire) of the national hydrological services equipped with an early version of the INRAE streamgauging ruler model. The reference measurements were obtained by various instruments routinely used and verified by these services: ADV Vectrino in the laboratory, various types of currentmeters in the field. The depth-averaged velocity to be compared with the streamgauging ruler velocity was established using standardized approaches (ISO748:2009, 2009): formulas for 1 or several points over the vertical, numerical integration of a vertical profile, or the depth-integrative method.

We brought together all of these 212 velocity comparisons carried out in the laboratory and in the field (Pernot, 2018). Our data cover a depth range of 5–55 cm and a velocity range of 0–75 cm/s. Through linear regression, we obtained a velocity rating that is very close to that of Pike et al. (2016):

$$V = 0.631\sqrt{2g\Delta h} - 0.009 \qquad (R^2 = 0.94) \tag{5}$$

Note that near-zero velocity results due to negligible velocity-heads were discarded as non significant and not used in the determination of the velocity rating. This velocity rating was established with a dataset about ten times smaller than that of Pike et al. (2016). As their rating fits our comparison data just as precisely (Fig. 4), with a negligible velocity bias of around 1%, there is no reason to question it and replace it. On the contrary, our data confirm their velocity rating, therefore we decided to keep using Eq. (3) in all our applications. We find an RMSE (0.051 m/s) similar to what they found (0.06 m/s). Note that the velocity rating assigns a slightly negative velocity to points corresponding to $\Delta h = 0$. For simplification, any negative velocity will be replaced by zero in further computations.

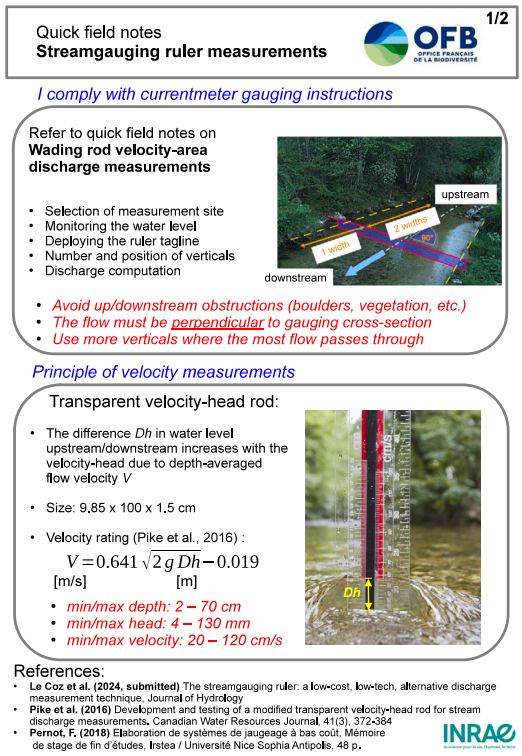

(a)

Streamgauging ruler measurement — Discharge (L/s): 98.9

Operators:	Clément, Maxime	Date:	21/04/2022
Stream Name:	La Liepvrette	Site Name:	Liepvreville
Rod ID:	2107	Start Bank (Left/Right):	Right
START Time:	08:20 UTC+2	END Time:	08:30 UTC+2
START Water Level (cm):	9.5	END Water Level (cm):	9.5

Vertical	Position (m)	Flow depth (cm)	Velocity head (mm)	Edge coefficient	Observations
1	1.88	15		0.67	
2	2.06	18.5	6		
3	2.17	20	6		
4	2.27	24	13		
5	2.38	30	8		
6	2.49	34.5	9		
7	2.6	34.5	3		
8	2.71	33.5	6		
9	2.82	35	3		
10	2.93	34	2		
11	3.04	34	10		
12	3.15	34	10		
13	3.26	28.5	21		
14	3.42	15	6		
15	3.6	12		0.86	

(b)

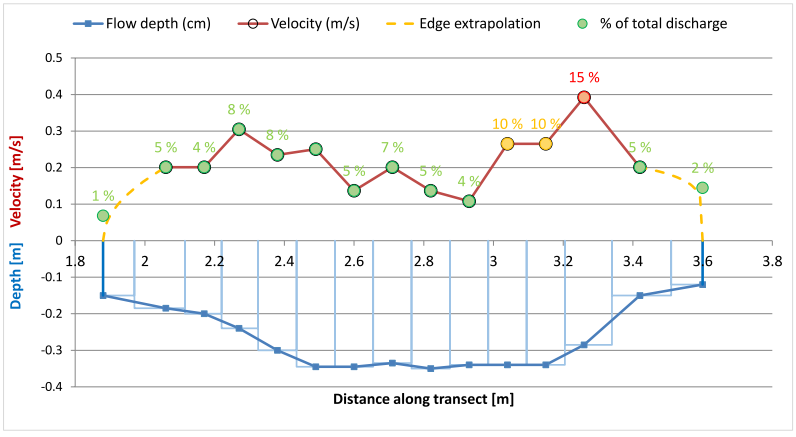

(c)

Fig. 3. Practical tools for streamgauging ruler measurements (provided in the supplementary materials): (a) OFB/INRAE brief field procedure, (b) field measurements and (c) results visualization in the INRAE spreadsheet.

3.2. Velocity measurement errors

Various sources of error can affect the velocity determined using a streamgauging ruler. The factors influencing velocity errors are important to study in order to assess the quality of the results and to quantify the measurement uncertainty. Over all the comparison data, the relative deviation of the rated velocity from the depth-averaged velocity reference (or "rated velocity error") does not seem to depend on the flow depth of the measurement vertical (Fig. 5a).

On the other hand, rated velocity errors sharply increase with decreasing velocity (Fig. 5b). While the data are scarce for velocities higher than 0.6 m/s, the increase of velocity errors for velocities lower than 0.20 m/s is obvious. This range corresponds to water level differences Δh less than about 5 mm. The most likely reason is the increasing sensitivity of the rated velocity to ruler and slider positioning errors and to velocity-head reading errors. For instance, the velocity rating (Eq. (3)) implies that a +1 mm error in Δh creates relative velocity errors of +22% and +40% for Δh = 3 mm (0.13 m/s) and Δh = 2 mm (0.09 m/s), respectively. As a result, for flow velocities lower than 0.4 m/s, velocity errors can be much higher than 10%. However, discharge errors may be lower, as random errors average out

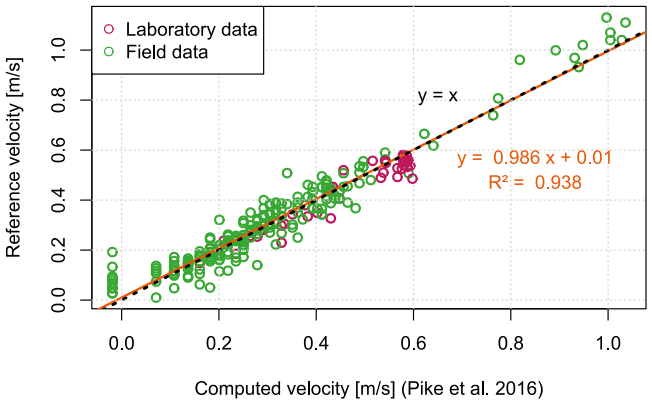

Fig. 4. Confirmation of the velocity rating (Eq. (3)) proposed by Pike et al. (2016) with comparison data from Pernot (2018). Slightly negative velocity points (due to zero velocity-head values) were excluded from the linear regression.

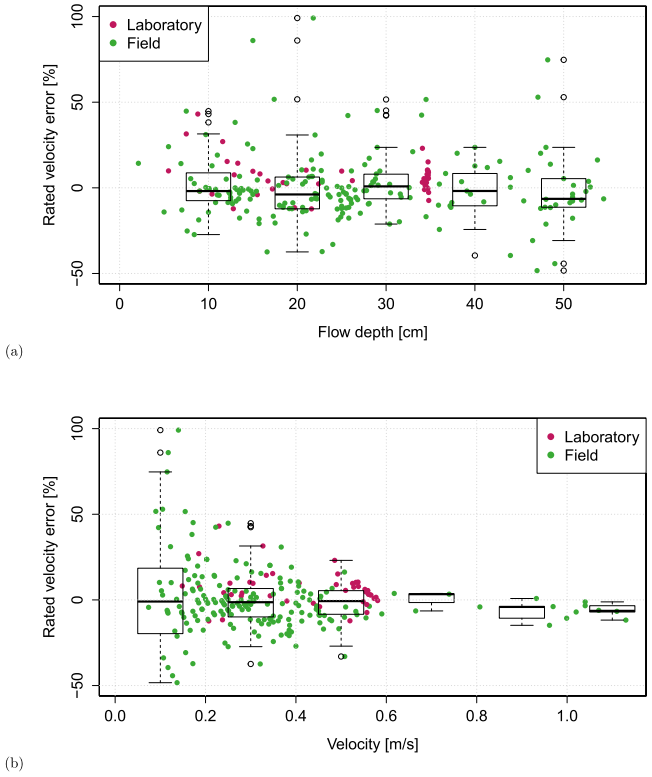

Fig. 5. Streamgauging ruler velocity errors versus (a) flow depth reference and (b) flow velocity reference. Laboratory and field data are displayed along with boxplots computed over equally-spaced intervals. Sixteen low-velocity data with rated velocity errors greater than 100% in absolute value are not shown on these plots but included in the boxplot computations.

in the spatial integration over the cross-section. Discharge errors are studied in the next section.

3.3. Discharge measurement errors

Fig. 6 presents the results of 97 discharge comparison tests collected in France, Costa Rica and Austria by various operators since the first models of streamgauging ruler have been released in 2018 (cf. data in Table 1). Such discharge comparisons are important to evaluate the final performance of the technique for various site and flow conditions, and to ensure the comparability of discharge results with more traditional and accepted measuring techniques.

The concurrent streamgauging techniques are usually currentmeters (any type) mounted on a wading rod, acoustic Doppler current profilers (ADCP), along with a few salt dilution and video based discharge measurements. When several concurrent techniques have been deployed, the average result is taken as the reference. Most of the data presented here have been created by relatively experienced field hydrologists, which means that errors due to site selection, instrument deployment, distribution of the verticals, etc. are minimized. This ensures that the discharge reference uncertainty is typical of good conditions, i.e. less than 10% usually. Comparison data are more scarce for very slow flows since beforehand, we advised the testing users avoiding these conditions.

As already observed by Pike et al. (2016) (with other data) and Pernot (2018) (with a subset of our dataset), most (76% in this dataset) streamgauging ruler discharges with section-averaged velocity greater than 0.2 m/s deviate from reference discharges by less than 10% in absolute value. Overall, out of all the 97 discharge comparisons, 71% and 94% have discharge errors smaller than 10% and 20%, respectively. The mean discharge deviation (or bias) and the mean absolute deviation are +0.1% and 7.8%, respectively.

A Gaussian distribution of discharge errors was estimated with the R package of GAMLSS (Generalized Additive Models for Location, Scale and Shape, https://www.gamlss.com/). The mean μ of the Gaussian distribution was assumed to be a linear function of V, the section-averaged velocity, and the standard-deviation σ was assumed to be a linear function of $1/V$, to capture the visible increase of errors for lower velocity. The mean error μ remains less than 0.5% in absolute value ($\mu = -0.0157V + 0.00815$), suggesting that the bias of the streamgauging ruler technique is negligible. As expected, the standard deviation σ increases when velocity decreases ($\sigma = 0.0118/V + 0.0520$), exceeding the 10% interval for $V = 0.2$ m/s, approximately. Note that this standard deviation is greater than the streamgauging ruler discharge uncertainty, as it includes the variability due to the measurement uncertainty of the reference discharges. There are too few data for velocity higher than 0.5 m/s to ensure that the discharge uncertainty does not increase for high velocity, especially when the flow depth is small and the streambed is coarse and uneven. In such conditions, the discharge measurement could be substantially biased.

4. Error sources and uncertainty analysis

4.1. Discharge uncertainty computation

The GUM (JCGM 100:2008, 2008) provides a widely accepted framework for computing measurement uncertainty from the Data Reduction Equation (DRE), i.e. the equation used to compute the measurand, here the discharge, from elemental measurements. For streamgauging ruler discharge measurements, the DRE is Eq. (4) with additional correction factors accounting for "hidden" errors such as instrument calibration errors and discharge interpolation errors between the verticals (and the edges). The ISO748 standard (ISO748:2009, 2009) and the Hydrometric Uncertainty Guide (ISO/TS25377:2007, 2009) propose similar uncertainty propagation equations for velocity-area gaugings, which are derived from a DRE similar to Eq. (4). Following the same principles, the relative (i.e. percentage) standard discharge uncertainty for a streamgauging ruler measurement can be established as:

$$u'^2(Q) = u'^2_s + u'^2_m + \sum_{i=0}^{m+1} \frac{Q_i^2}{Q^2} \left(u'^2_{B_i} + u'^2_{D_i} + u'^2_{V_i} \right) \quad (6)$$

where u'_s is the uncertainty due to residual systematic errors of the system, u'_m is the uncertainty due to the lateral discharge integration errors, and u'_{B_i}, u'_{D_i} and u'_{V_i} are the width, depth and velocity measurement uncertainty terms, respectively. Total discharge Q is the sum of partial discharges $Q_i = B_i\ D_i\ V_i$ (cf. Eq. (4)).

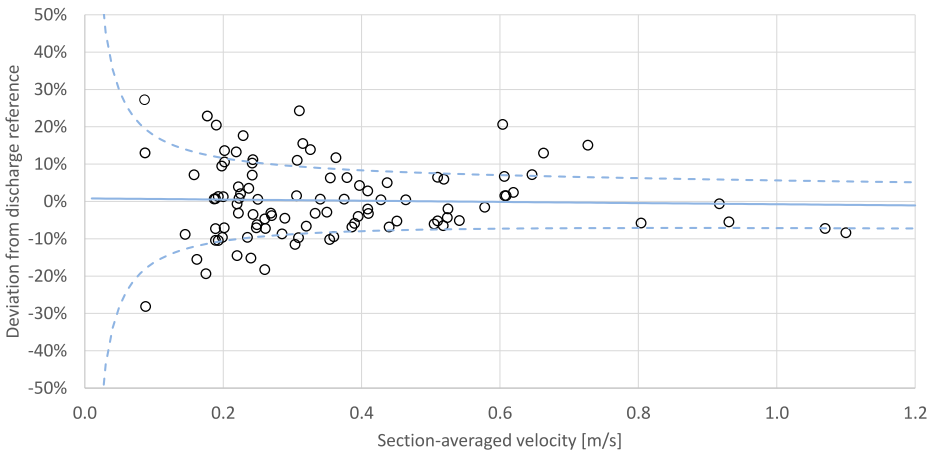

Fig. 6. Streamgauging ruler discharge deviations from discharge references versus section-averaged velocity for 97 streamgauging measurements taken by relatively experienced operators in various rivers and streams in France, Costa Rica and Austria (circles). The solid and dashed lines are, respectively, the mean and the ±1 standard deviation envelope around the mean of a Gaussian distribution of errors estimated with GAMLSS (see text for details).

Those uncertainty terms are estimated based on the following assumptions, open to further revisions when better estimates are available. As usually assumed for currentmeters (Le Coz et al., 2012), u'_s = 1%.

The lateral discharge integration errors are determined not only by the number of verticals, as assumed by the ISO748 method, but also by the complexity of the cross-sectional geometry and flow, which have to be sampled laterally (Despax et al., 2016). This motivated the development of several alternative methods, e.g. IVE (Cohn et al., 2013), Q+ (Le Coz et al., 2012, 2015) and Flaure (Despax et al., 2016), to estimate u'_m (for an introduction and comparison of those methods, see Despax et al., 2016). For comparison, the ISO748, Q+ and Flaure methods were implemented in the discharge computing spreadsheet (the IVE will be added later).

For the ISO748 method, the interpolation of the u'_m values specified by the standard is done using the fit proposed by Le Coz et al. (2012):

$$u'_m = 32\ m^{-0.88} \tag{7}$$

where m is the number of verticals.

In the Q+ method, u'_m is computed as:

$$u'^2_m = \sum_{i=0}^{m+1} \frac{Q_i^2}{Q^2} \left(u'^2_{m,D_i} + u'^2_{m,V_i} \right) \tag{8}$$

where the depth and velocity lateral integration uncertainty components, respectively u'_{m,D_i} and u'_{m,V_i}, are computed as explained by Le Coz et al. (2012, 2015). As a conservative assumption, the maximum bed variation angle is arbitrarily set as $\alpha = 15°$.

Last, a simplified version of the Flaure method (Despax et al., 2017) is used to compute u'_m as a second-order polynomial function of the Sampling Quality Index (SQI) η introduced by Despax et al. (2016) (see their equation 19):

$$u'_m = -0.059\ \eta^2 + 0.214\ \eta + 0.003 \tag{9}$$

Since this equation was calibrated from data with $\eta < 1.2$, u'_m is kept constant for higher values of the SQI: $u'_m = 17.5\%$ if $\eta \geq 1.2$.

From our experience with the streamgauging ruler, the width and depth measurement errors seem constant in absolute length rather than proportional. To compute u'_{B_i} and u'_{D_i} at each vertical, we assume that the absolute standard uncertainty is 0.01 m for width and 0.005 m for flow depth. The latter value is similar to the depth measurement standard uncertainty (0.0047 m) quantified by Pike et al. (2016). However, the flow depth uncertainty might be greater for high velocities due to the bow wave created by the board.

The results of our evaluation tests (cf. Section 3.2) suggest that most of the velocity uncertainty, u'_{V_i}, is due to velocity-head reading errors. This uncertainty component will be modeled in the next section. As the streamgauging ruler directly measures the depth-averaged velocity, the vertical velocity integration error is ignored (no such uncertainty component as u_p in the ISO748, Q+, Flaure methods). In the near-edge half-panels ($i = 0$ and $i = m + 1$), the velocity is computed as the product of the nearest velocity measurement and $2C_i - 1$, with C_i the edge coefficient. Therefore, the velocity in the near-edge coefficient is computed as:

$$\begin{cases} u'^2_{V_0} &= u'^2_{V_1} + u'^2_{C_0} \\ u'^2_{V_{m+1}} &= u'^2_{V_m} + u'^2_{C_{m+1}} \end{cases} \tag{10}$$

Similar to the method of Le Coz et al. (2012), C_i is assumed to follow a uniform distribution bounded by extreme values 2/3 and 10/11, which induces that the relative standard deviation is $u'_{C_0} = u'_{C_{m+1}} = 9\%$.

The expanded (95% probability level) discharge uncertainty $U'(Q) = k \times u'(Q)$ is expressed with a coverage factor $k = 2$. The usual justification of such metrological practice is that discharge errors are assumed normally-distributed and that the half-width of the 95% confidence interval of a Gaussian distribution is equal to 1.96 times the standard-deviation (1.96 is rounded up to 2).

4.2. Velocity uncertainty analysis

Assuming that velocity reading errors are dominant, we need to compute the velocity uncertainty u'_{V_i} using an equation that reflects both the effects of resolution (or limited sensitivity) and water level pulsations. Resolution errors increase with decreasing velocity while the magnitude of water level pulsations increases with increasing velocity. Applying the uncertainty propagation method of the GUM (JCGM 100:2008, 2008) to Eq. (3) yields the following expression of the relative velocity uncertainty u'_{V_i} due to resolution errors:

$$u'_{V_i} = \frac{\delta}{2\Delta h_i} \tag{11}$$

with δ the 95% expanded velocity-head uncertainty due to the resolution and adjusting errors of the rulers (we assume δ = 1 mm thereafter).

A purely empirical uncertainty component is added to reflect the effect of water level fluctuations which increase with velocity. This uncertainty component is assumed to be proportional to flow velocity (and therefore to $\sqrt{\Delta h}$ according to Eq. (3)) with a coefficient γ evaluated empirically ($\gamma = 0.1\ \mathrm{m}^{-1/2}$):

$$u'_{V_i} = \sqrt{\frac{\delta^2}{4\Delta h_i^2} + \gamma^2 \Delta h_i} \tag{12}$$

Table 1
Results of the discharge comparison tests collected since 2018 and displayed in Fig. 6.

				Streamgauging ruler results			Reference		
	River	Site	Country	Wetted area [m²]	Mean velocity [m/s]	Discharge [m3/s]	Discharge [m3/s]	Error [%]	Absolute error [%]
1	Ru d'Homède	Homède	France	1.000	0.087	0.087	0.068	+27%	27%
2	Homède	Creissels	France	1.000	0.087	0.087	0.077	+13%	13%
3	Les deux Fonds	Avoise	France	2.420	0.088	0.212	0.295	-28%	28%
4	Orge	Saint Chéron	France	1.139	0.145	0.165	0.181	-9%	9%
5	Quebrada Máquinas		Costa Rica	0.705	0.158	0.112	0.105	+7%	7%
6	Claduègne	ancien pont RN102	France	0.788	0.162	0.128	0.152	-16%	16%
7	Mare	Vérines	France	0.448	0.175	0.078	0.097	-19%	19%
8	Charreau	Voeuil et Giget	France	1.610	0.177	0.285	0.232	+23%	23%
9	Claduègne	ancien pont RN102	France	0.802	0.187	0.150	0.149	+1%	1%
10	Homède	Creissels	France	0.362	0.189	0.069	0.077	-10%	10%
11	Petit Morin	Montmirail	France	1.758	0.189	0.332	0.358	-7%	7%
12	Ru d'Homède	Homède	France	0.362	0.189	0.069	0.068	+1%	1%
13	Argence	Champniers	France	1.980	0.190	0.377	0.313	+20%	20%
14	Aubetin	Le Poncet	France	2.580	0.193	0.497	0.555	-10%	10%
15	Claduègne	ancien pont RN102	France	0.800	0.193	0.154	0.152	+1%	1%
16	Céor	Cassagnes-Bégonhes	France	1.050	0.198	0.208	0.190	+9%	9%
17	Adour de Payolle	AP4	France	1.240	0.199	0.249	0.276	-10%	10%
18	Ozon	Chatellerault Moulin	France	2.270	0.200	0.470	0.464	+1%	1%
19	Largue	Pont de Lincel (S2)	France	1.246	0.201	0.251	0.270	-7%	7%
20	Rupt-de-Mad	Richecourt	France	1.570	0.202	0.317	0.279	+14%	14%
21	Ratier	aval station	France	0.059	0.202	0.012	0.011	+11%	11%
22	Claduègne	ancien pont RN102	France	0.741	0.219	0.162	0.143	+13%	13%
23	Exutoire du lac	Radonvilliers	France	1.380	0.220	0.301	0.303	-1%	1%
24	Ecole	Dannemois	France	1.950	0.220	0.436	0.510	-15%	15%
25	Durzon	Pont du Mas	France	2.370	0.222	0.525	0.542	-3%	3%
26	Durzon	Pont du Mas	France	2.850	0.222	0.634	0.610	+4%	4%
27	Durzon	Pont du Mas	France	2.760	0.223	0.615	0.610	+1%	1%
28	Taude	Saint Brice	France	0.219	0.225	0.049	0.048	+2%	2%
29	Razes	Station	France	0.009	0.229	0.0020	0.0017	+18%	18%
30	Berdin	Tennie	France	0.482	0.235	0.113	0.125	-10%	10%
31	Durzon	Pont du Mas	France	2.370	0.237	0.561	0.542	+4%	4%
32	Exutoire du lac	Radonvilliers	France	1.050	0.240	0.257	0.303	-15%	15%
33	Durzon	Pont du Mas	France	2.630	0.242	0.636	0.594	+7%	7%
34	Durzon	Pont du Mas	France	2.710	0.242	0.655	0.594	+10%	10%
35	Rupt-de-Mad	Richecourt	France	1.310	0.243	0.318	0.286	+11%	11%
36	Largue	Pont de Lincel (S1)	France	0.985	0.243	0.239	0.248	-3%	3%
37	Tholon	Senan	France	0.690	0.248	0.171	0.184	-7%	7%
38	Roule-Crotte	Arnage Gué Gilet	France	0.488	0.249	0.121	0.129	-6%	6%
39	Nouère	Asnières	France	1.430	0.250	0.356	0.354	+1%	1%
40	Gave d'Azun	GA4	France	3.460	0.260	0.907	1.110	-18%	18%
41	Gée	Fercé Planche Augis	France	1.099	0.260	0.285	0.299	-5%	5%
42	Tributary of Río Rastra		Costa Rica	0.437	0.261	0.114	0.123	-7%	7%
43	Gée	Fercé Planche Augis	France	1.034	0.269	0.278	0.287	-3%	3%
44	Exutoire du lac	Radonvilliers	France	1.560	0.270	0.424	0.441	-4%	4%
45	Céor	Castelpers	France	0.664	0.285	0.189	0.207	-9%	9%
46	Charbonnières	aval station Casino	France	0.117	0.289	0.034	0.036	-4%	4%
47	Liesing	Vienna	Austria	0.697	0.304	0.212	0.240	-12%	12%
48	Roule-Crotte	Arnage Gué Gilet	France	1.080	0.306	0.330	0.325	+2%	2%
49	Grande rivière	Digue AEP	France	3.620	0.307	1.110	1.000	+11%	11%
50	Viaur	Saint-Just	France	7.220	0.309	2.230	2.470	-10%	10%
51	La Veude	Lémeré	France	1.560	0.310	0.486	0.391	+24%	24%
52	Argentor	Poursac	France	1.490	0.315	0.469	0.406	+16%	16%
53	Exutoire du lac	Radonvilliers	France	0.890	0.320	0.283	0.303	-7%	7%
54	Tributary of Río		Costa Rica	0.113	0.326	0.037	0.032	+14%	14%
55	Liesing	Vienna	Austria	0.697	0.333	0.232	0.240	-3%	3%
56	Morgon	Villefranche	France	0.840	0.340	0.286	0.284	+1%	1%
57	La Trezence	Puyrolland	France	0.780	0.350	0.270	0.278	-3%	3%
58	Bonnieure	St Ciers	France	2.370	0.354	0.839	0.934	-10%	10%
59	Quebrada AL1 (Lago		Costa Rica	0.044	0.355	0.016	0.015	+6%	6%
60	Négron	Beuxes	France	0.390	0.360	0.134	0.148	-9%	9%
61	Dourbie	Cantobre	France	5.180	0.363	1.880	1.683	+12%	12%
62	Adour	AD1	France	3.550	0.375	1.336	1.328	+1%	1%
63	Durzon	Pont du mas	France	3.340	0.379	1.266	1.190	+6%	6%
64	Azergues	Châtillon	France	5.98	0.39	2.31	2.480	-7%	7%
65	Voulzie	Jutigny	France	3.280	0.390	1.280	1.360	-6%	6%
66	Le Tillet	Aix-les-Bains	France	1.945	0.395	0.788	0.821	-4%	4%
67	Rupt-de-Mad	Euvezin	France	2.420	0.397	0.961	0.922	+4%	4%
68	Azergues	Châtillon	France	6.240	0.409	2.550	2.480	+3%	3%
69	Adour de Gripp	AG1	France	0.797	0.409	0.338	0.345	-2%	2%
70	Azergues	Châtillon	France	5.860	0.410	2.400	2.480	-3%	3%
71	Sausseron	Nesles-la-Vallée	France	1.039	0.428	0.444	0.442	+0%	0%
72	Canal des Albères	Prise d'eau	France	0.811	0.437	0.354	0.337	+5%	5%
73	Exutoire du lac	Radonvilliers	France	2.370	0.440	1.050	1.127	-7%	7%
74	Ardières	Pizay	France	4.410	0.451	1.990	2.100	-5%	5%
75	Grand Morin	Meilleray	France	2.388	0.464	1.108	1.103	+0%	0%
76	Javel	Amont stade	France	0.277	0.505	0.140	0.149	-6%	6%
77	Arguenon	Jugon les Lacs – Bois	France	2.860	0.510	1.460	1.540	-5%	5%
78	Exutoire du lac	Radonvilliers	France	2.360	0.510	1.200	1.127	+6%	6%
79	Javel	Amont stade	France	0.278	0.518	0.144	0.154	-6%	6%
80	Adour de Payolle	AP1	France	1.630	0.519	0.862	0.814	+6%	6%
81	Ouvèze	Vaison. pont romain	France	1.320	0.524	0.662	0.692	-4%	4%
82	Río Alondra		Costa Rica	0.305	0.525	0.160	0.163	-2%	2%
83	Arvon aval	Source	France	1.539	0.541	0.833	0.878	-5%	5%
84	Durzon	Pont du mas	France	3.340	0.578	1.930	1.960	-2%	2%
85	Dourbie	Cantobre	France	3.360	0.604	2.030	1.683	+21%	21%
86	Lez	Source	France	4.400	0.606	2.668	2.500	+7%	7%
87	Durzon	Pont du mas	France	3.280	0.607	1.990	1.960	+2%	2%
88	Durzon	Pont du mas	France	3.270	0.609	1.990	1.960	+2%	2%
89	Lez	Source	France	6.616	0.619	4.097	4.000	+2%	2%
90	Lez	Source	France	5.010	0.646	3.238	3.021	+7%	7%
91	Galamache	Haute-Vienne	France	0.908	0.663	0.602	0.533	+13%	13%
92	Rupt-de-Mad	Euvezin	France	1.870	0.727	1.360	1.182	+15%	15%
93	Gave de Gavarnie	GG3	France	2.450	0.804	1.980	2.101	-6%	6%
94	Drac	Chabottes	France	1.680	0.917	1.550	1.560	-1%	1%
95	Vaige	Bouessay	France	0.315	0.931	0.294	0.311	-5%	5%
96	Petit canal	Lac de Seine	France	0.455	1.070	0.487	0.525	-7%	7%
97	Petit canal	Lac de Seine	France	0.437	1.100	0.481	0.525	-8%	8%
							Mean	0.1%	7.8%

With these assumptions, the velocity uncertainty is lowest for flow velocity between 40 and 60 cm/s (cf. Fig. 7). The velocity expanded uncertainty exceeds 10% (i.e. $u'_{V_i} > 5\%$) when the flow velocity is lower than 20 cm/s (the resolution/adjustment uncertainty dominates) or faster than 1.4 m/s (uncertainty due to level fluctuations dominates), i.e. beyond the velocity range over which calibration data for the velocity rating exist. The uncertainty model of Eq. (12) confirms our experience (cf. Figs. 5b and 6) that the poor sensitivity of the streamgauging ruler for low velocities is more detrimental than water level fluctuations occurring at high velocity. However, the assumptions and values retained empirically should be confirmed by further studies.

4.3. Examples of discharge uncertainty results

The aforementioned uncertainty computation is implemented in the spreadsheet proposed for streamgauging ruler measurements. For each of the ISO748, Q+ and Flaure methods, the spreadsheet displays the 95% expanded, relative discharge uncertainty $U'(Q)$ in percentage of measured discharge Q along with the uncertainty budget, in which the contribution of each uncertainty component is expressed as a percentage of the total variance $u'^2(Q)$. For instance, the share of the uncertainty due to systematic errors is expressed as $u'^2_s/u'^2(Q)$, and the share of the width measurement uncertainty is expressed as

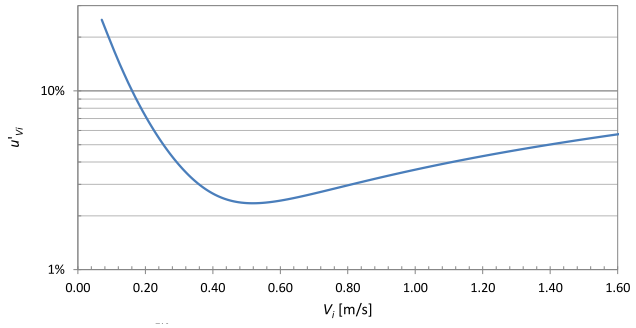

Fig. 7. Velocity standard uncertainty u'_{V_i} estimated using Eq. (12) versus flow velocity V_i.

$\sum_{i=0}^{m+1}(Q_i^2/Q^2)u'^2_{B_i}/u'^2(Q)$. Similar expressions are used to compute the shares of the depth measurement uncertainty, velocity-head reading uncertainty, edge coefficients uncertainty, and lateral integration uncertainty, the latter being split into depth and velocity lateral integration uncertainty components in the Q+ method.

The examples shown in Fig. 8 illustrate the discharge uncertainty results obtained for a range of measuring conditions based on a real, typical streamgauging ruler measurement performed in good conditions (cf. Fig. 8a): optimal velocity range (around 40 cm/s) and 14 verticals well distributed across the stream (partial discharges are all lower than 10% of total discharge). This measurement was conducted in the Azergues River at Châtillon d'Azergues (hydrometric station U4624010) on 26/01/2023 from 09:46 to 10:08 UTC+1 (stage read at staff gauge 0.335 m, no variation). Typical of the uncertainty expected for a good streamgauging ruler measurement, the discharge uncertainty estimates (7%–8%) are in close agreement across the three methods. The Q+ variance budget is dominated by lateral integration uncertainty components, which means that the discharge uncertainty could be further decreased by increasing the number of verticals.

To illustrate the behavior of the uncertainty computation, three virtual examples are created from this real measurement to simulate poorer conditions: very few verticals, very low velocities, and very high velocities. First, only 1 vertical out of 3 is kept to get a number of verticals as low as 4 (cf. Fig. 8b). Obviously, partial discharges are too high (up to 35% around the deepest vertical). The discharge uncertainty estimated by ISO748 method is high (19%), while Q+ and Flaure uncertainty estimates are different and even higher (29%–31%). Differences are due to the different approaches to estimate the lateral integration uncertainty components, which dominate the variance budget.

Then, in the initial measurement with 14 verticals, velocity-head values are divided by 15 so that nearly all velocity measurements are slower than 10 cm/s (cf. Fig. 8c). Now the dominant uncertainty source is velocity head reading uncertainty, computed with the same equation in all three uncertainty methods, so that they yield similar discharge uncertainty estimates (21%–22%). Such higher uncertainty reflects the impact of the resolution errors highlighted in Section 3.2.

Last, velocity-head values are multiplied by 5 so that most velocity measurements are higher than 90 cm/s, with a maximum around 125 cm/s (cf. Fig. 8d). The uncertainty estimates (7%–8%) remain as low as in the initial measurement and the variance budget is still dominated by lateral integration uncertainty components, suggesting that water level fluctuations for high velocities do not significantly increase the velocity and discharge uncertainty.

5. Discussion

5.1. A cost-efficient streamgauging tool for all

The streamgauging ruler, i.e. the transparent velocity-head rod model we have proposed, has proved to be reliable when used in good conditions, which mainly means well-trained operators and flow velocity greater than 20 cm/s for the majority of the stream. Then, the reported discharge differences from accepted references are usually within 10%, which is acceptable for many purposes. The reason why we observe a better performance than Davids et al. (2019) and King et al. (2022) is not obvious, as it could be a better instrument design, a more accurate velocity rating (the equation established by Pike et al. (2016) from many field observations rather than the relation established from flume calibration by Hundt and Blasch (2019) or the uncorrected velocity-head equation used by Davids et al. (2019)), a better field deployment and training, or a combination of these factors.

As of July 2024, 304 streamgauging rulers had been built by us or by AAIS, and released to academic and professional users around the world (cf. the locations of users around the world on this map[2]). News and new versions of the spreadsheet are released through a webpage[3] and a user mailing-list with more than 200 members. A smartphone application Qraj based on QField[4] has been developed by the CATER Calvados Orne Manche association[5]: similar to the spreadsheet, Qraj will make field measurements easier. In France, the streamgauging ruler has been increasingly used by professionals not specialized in hydrometry, i.e. technicians from river boards, irrigation boards, environmental regulation agencies, etc. Several hydrometry services also use it for comparisons and sharing experience with their partners. The shortest (60 cm-long) model of the streamgauging ruler is used by cavers of the French Federation of Speleology. The potential for citizen science programs (Davids et al., 2019) is high, of course, and also for teaching students (Fonstad et al., 2005), for the development of low-income countries, and for engaging with the general public on hydrometric culture. The simplicity of the instrument makes it a good tool to focus on the basic knowledge of streamgauging instead of instrument-specific details: safety rules, site selection, flow steadiness, number and positions of the verticals, measurement repeatability and uncertainty, discharge computation, ... and the great value of hydrological data!

5.2. Advantages and limitations

Beyond its relatively good accuracy, the main advantages of the instrument are its low price (low-cost), of course, but also its low technological level (low-tech): the instrument and spreadsheet can be handled by any operator after a very short training (less than one hour) using the video tutorial; the physical elements of the instrument are sturdy, easily fixed, built or replaced, with no power supply or electronic devices; the instrument is relatively small and lightweight, hence easily stored (in a vehicle for instance) and carried to remote sites, including underground streams and caves. The discharge measurement is much quicker than with a currentmeter or floats because only one measurement per vertical is required to get the depth-averaged velocity, whereas several velocity points might be measured when using a currentmeter (depending on the field procedure) and the float injections are often repeated 2 or 3 times, for repeatability (Le Coz et al., 2011). In addition, the adjustment of the rulers by an experienced operator is usually quicker than the required time of exposure of currentmeters (30–40 s, typically ISO748:2009, 2009) or than the traveling time of floats along the required distance (20 m, typically Le Coz et al., 2011). Compared to floats, the streamgauging ruler is insensitive to wind and does not require adjusting a flow-specific surface to depth-average velocity coefficient (but floats can be used in very slow flows).

[2] https://www.google.fr/maps/@16.2323975,-55.7504603,4z/data=!4m2!6m1!1s1xiIfwv6PItw7nNAVwD0unEE1Ii5JYWY?hl=en&entry=ttu.

[3] https://riverhydraulics.riverly.inrae.fr/eng/tools/instrumentation/streamgauging-rulers.

[4] https://qfield.org/.

[5] https://www.cater-com.fr/.

Fig. 8. Uncertainty estimates for (a) a typical streamgauging ruler discharge measurement in good conditions, and the same measurement with (b) 2 verticals out of 3 removed, (c) reduced velocity, (d) increased velocity.

Currentmeters (any type) require a minimum flow depth to immersed (3–4 times their vertical size, typically, cf. ISO748:2009, 2009), a requirement often overlooked by practitioners, resulting in biased velocity measurements. The streamgauging ruler can be used in very shallow flows (down to a few centimeters) where other instruments cannot be used. For instance, broad-crested weirs are very good measuring cross-sections for the streamgauging ruler to get velocity high enough, perpendicular flow field, and stable, flat streambed. Non-uniform vertical velocity profiles on a weir are not a problem as the streamgauging ruler directly integrates the velocity over the flow depth.

The main limitation of the streamgauging ruler is its limited sensitivity to low velocity. Since the beginning, Wilm and Storey (1944) stated that the instrument was "inaccurate for velocities much below 1 ft per sec" (about 30 cm/s). It is unclear whether such limitation

could be improved or not, e.g. by modifying the design of the instrument. Our preliminary attempts to increase the sensitivity using wider boards or semi-circular gutter, thus increasing the drag, were not encouraging. As also mentioned by Wilm and Storey (1944), "streams with soft, unstable beds" are an issue (same problem as with any wading rod streamgauging technique), which might be solved by adding a removable, flat stand to the board. Such a stand would also help handling the instrument in fast flows (some users place one of their feet behind the board). To measure the incident angle of oblique flows, a protractor could be adjusted on the flat side of the board, and the velocity projection could be implemented in a future version of the spreadsheet. The ergonomic design of the instrument could certainly be improved, notably so that the operator does not have to bend over shallow flows. Solutions based on some electrical contact activating a buzzer or a light when the tip of a ruler touches the water surface have been considered and tested. However, the low-cost and low-tech qualities of the system should be preserved.

5.3. Physical explanation for the velocity rating

A more fundamental question is what is the exact velocity sampling volume and why does the theoretical velocity rating (Eq. (1)) need to be corrected as shown by Fonstad et al. (2005), Pike et al. (2016) and us through semi-empirical velocity rating equations (Eqs. (2) and (3)) calibrated from field comparison data.

Surprisingly, previous authors using Eq. (1) did not report any observed bias in their comparison data. For instance, Wilm and Storey (1944) found that their velocity-head rod discharges were in acceptable agreement with their discharge references from calibrated structures, with no obvious bias. However, Heede (1974) found that the mean ratio between velocity-head rod discharge measurements in a boulder-strewn stream and a San Dimas flume taken as a reference was 1.65 ± 0.08 with a confidence level of 95%. He attributed such overestimating bias to depth overestimation when the board could not be maintained at the top of slippery boulders, and to "incomplete conversion of velocity head to depth" due the flow lines complexity and unsteadiness (the latter effect being opposite to velocity overestimation, surprisingly). Actually, he might have realized the need for a velocity rating correction later discovered by Fonstad et al. (2005), since the inverse of the mean discharge bias he observed ($1/1.65 = 0.61$) is close to the velocity correction factors in Eqs. (2) and (3).

Fonstad et al. (2005) proposes three reasons for the measured water surge Δh to be higher than predicted by the theoretical velocity rating (Eq. (1)). First, the surge upstream of the board would be mainly created by near-surface flow, which is faster than the depth-average flow. This is also what Hundt and Blasch (2019) concluded from their laboratory flume evaluation of a narrower velocity-head rod model, as they found a higher correlation of uncalibrated velocities (Eq. (1)) with velocities in the top 5 cm layer than with velocities in other layers of the flow. However, this would not explain a correction by a factor of about 0.64 as in Eq. (3), as the depth-average to surface velocity ratios (or "alpha coefficients") in fairly uniform river flows typically ranges from 0.8 to 0.9 (Hauet et al., 2018). Moreover, alpha coefficients can vary over a much wider range (0.6–1.2, typically, Le Coz et al., 2010; Welber et al., 2016) than the scatter observed in the comparison dataset of Pike et al. (2016) or ours. And the whole water column from bed to surface is blocked by the board so that it is unclear that the streamgauging ruler is more sensitive to near-surface flow than to the depth-average flow. Second, Fonstad et al. (2005) point out that Δh is measured from the slightly depressed water surface downstream of the board rather than from the undisturbed water surface. In practice, the drawdown is limited to a very small portion of Δh even for higher velocities.

Last, they explain that the measured superelevation is the maximum height while the mean over all the flow particles blocked by the board would be "a truer measure of potential energy". One may argue that the maximum superelevation measured at the center of the board should be a measure of the potential energy of the local flow, fully blocked by the obstacle. The superelevation is usually nearly constant across most of the board width and rapidly decreases beyond the board edges on both sides, where water is evacuated downstream. The excess flow around the board is not freely evacuated but controlled by the flow conditions downstream of the board, determined by the normal flow depth and local energy dissipation in the lee of the board.

While such speculation on the physical process behind the empirical velocity rating factors does not preclude the practical use of the velocity-head rods, understanding the physics could help improve the design and application of the system. It calls for high-resolution laboratory experiments and hydrodynamic studies, possibly including CFD simulations.

5.4. Improvement and validation of the uncertainty analysis

Pike et al. (2016) have identified and discussed various error sources in discharge measurements using a transparent velocity-head rod, such as the streamgauging ruler. Based on their results and our experience, in the uncertainty computation introduced in this paper, the errors in the determination of the velocity-head, due to both ruler adjustment and value reading, were considered as the main velocity uncertainty source. Of course, this assumption needs to be verified experimentally. The model (Eq. (12)) proposed for u'_{V_i} and the values of its parameters are based on our expert judgment. More detailed studies of these errors would be useful to evaluate and improve them.

From their extensive comparison of velocity measurements, Pike et al. (2016) quantified the velocity deviations around the mean velocity rating (with an RMSE of 0.06 m/s, similar to the RMSE we obtained, 0.051 m/s) and across several operators (with an operator-to-operator standard deviation of 0.016 m/s). The residuals around the velocity rating model are likely due to both the reading errors already counted in u'_{V_i}, and velocity reference errors, i.e. measurement errors of the FlowTracker currentmeter and of the 1-point method used to compute the depth-averaged velocity. Therefore, including the RMSE of 0.06 m/s in the streamgauging ruler uncertainty computation would lead to uncertainty overestimation and double-counting of the velocity-head reading uncertainty.

The operator-to-operator uncertainty may be due to personal biases in velocity-head reading, practical deployment (board angles and alignment), site selection, etc. Ideally, it should be included in the uncertainty computation, however we feel that further comparison experiments are needed to establish accurate uncertainty values valid across a broader range of operators and rivers, and using the newly developed model of streamgauging ruler. The spirit level and the top ruler graduation, in particular, hopefully decrease some operator-related errors in the board verticality and in the value readings. Because many streamgauging ruler users are not hydrometry experts, it would be interesting to quantify if operator-related errors are decreased through training, experience, and quality assurance/quality control (QA/QC). Such investigation could be conducted through repeated-measures experiments (or field intercomparison experiments) in variable site conditions as done by Le Coz et al. (2016) and Despax et al. (2019) for ADCP discharge measurements. Such experiments would be a practical means to evaluate the uncertainty computation method (Despax et al., 2023).

6. Conclusion

The modern version of the velocity-head rod modified by Fonstad et al. (2005) and Pike et al. (2016) and us is confirmed to be a cost-efficient and reliable streamgauging tool. The model developed by INRAE (the streamgauging ruler) is a little more expensive (commercially available independently from INRAE for about €210 VAT and shipping fees included) but it remains relatively easy to build and significantly improves the ease of use and the measurement quality.

Our laboratory and field comparison tests validate the velocity rating proposed by Pike et al. (2016). The main practical limitation is that velocity lower than about 20 cm/s cannot be measured precisely due to the limited sensitivity of the technique. Except for too slow flows, discharge measurements usually fall within ±10% from concurrent discharge estimates. The proposed uncertainty analysis method also suggests that, in good conditions, discharge uncertainty is of the order of 10%. The streamgauging ruler can be operated in very shallow flows (a few centimeters), which is an advantage over currentmeters.

An operator can be trained in less than half an hour and a streamgauging is significantly faster with a streamgauging ruler than with traditional methods such as currentmeters or floats. Typically, 15 verticals can be measured in about 15 min with a streamgauging ruler whereas it takes 2–3 times longer with a currentmeter measuring 2–3 velocity points per vertical. The technique is particularly recommended when the cost of the instrumentation and/or the technical skills of the operators are limiting, and when an uncertainty of the order of 10% is tolerable, e.g. for quick discharge estimation, training/education, citizen-science programmes, self-monitoring (e.g. irrigation boards), projects in developing countries, etc.

Research perspectives include the theoretical understanding of the velocity rating, and quantifying and reducing the operator-related errors, to be included in the uncertainty analysis of discharge measurements. Development perspectives include alternative designs to further improve the ergonomics and sensitivity to low flows, while keeping cost and complexity as low as possible. A new version of the spreadsheet for mobile devices is under development, and we would like to develop a smartphone application. Training an increasing number of operators, and getting feedback from them will certainly make the streamgauging ruler a popular and accepted streamgauging technique in the foreseeable future.

CRediT authorship contribution statement

J. Le Coz: Writing – review & editing, Writing – original draft, Supervision, Software, Project administration, Methodology, Investigation, Funding acquisition, Data curation, Conceptualization. **M. Lagouy:** Writing – review & editing, Resources, Methodology, Investigation, Data curation, Conceptualization. **F. Pernot:** Methodology, Investigation, Formal analysis, Data curation, Conceptualization. **A. Buffet:** Methodology, Investigation, Conceptualization. **C. Berni:** Writing – review & editing, Supervision, Methodology, Investigation, Data curation, Conceptualization.

Declaration of competing interest

The authors declare the following financial interests/personal relationships which may be considered as potential competing interests: Le Coz reports financial support was provided by French Biodiversity Office. Le Coz reports financial support was provided by French Ministry of Ecology. If there are other authors, they declare that they have no known competing financial interests or personal relationships that could have appeared to influence the work reported in this paper.

Data availability

Data will be made available on request.

Acknowledgments

We would like to thank all the field hydrologists who contributed to the validation of the streamgauging rulers by conducting comparative measurements, in particular Quentin Morice (DREAL Grand-Est), André Hébrard (DREAL Occitanie), Jocelyn Cousseau (DREAL Pays-de-Loire), Samuel André (DRIEAT Ile-de-France), Marie Degrave (DREAL Nouvelle-Aquitaine), Alexis Solignac (Fédération de l'Aveyron de Pêche et de Protection des Milieux Aquatiques), Guillaume Dramais, Mickaël Lagouy, Fanny Courapied, Adrien Bonnefoy and Benoît Camenen (INRAE), Guillaume Nord, Alexandre Hauet (IGE, Université Grenoble Alpes), Christophe Apolit (Parc Naturel Régional des Grands-Causses), Yvan Falatas, François-Xavier de Resseguier (OFB), Vincent Cornu (ECOGEA), Claire Bernard (Chambre d'agriculture de Vaucluse), Pierre Marchand (HydroSciences Montpellier), Erwan Le Barbu and Amélie Rzadkiewa (DREAL Bourgogne-Franche-Comté), Adrien Vergne (DREAL Bretagne), Claire Delus (Université de Lorraine), and all their colleagues. We also thank Robin Pike (British Columbia Ministry of Environment) for sharing his valuable thoughts, data, documents and advice with us. This work was supported by the French Office for Biodiversity (OFB) through INRAE-OFB contract CO-OFB 2022–24 (Hydro-DMB, Action 6) and by the Ministry in charge of Ecology through the program DGPR/SRNH-IRSTEA 2017 research programme (grant decision 2102049246).

Appendix A. Supplementary data

Supplementary material related to this article can be found online at https://doi.org/10.1016/j.jhydrol.2024.131887.

References

Biggs, H., Smart, G., Doyle, M., Eickelberg, N., Aberle, J., Randall, M., Detert, M., 2023. Surface velocity to depth-averaged velocity—a review of methods to estimate alpha and remaining challenges. Water (Switzerland) 15 (21).

Bureau, H., 1910. Nouvelle méthode de jaugeage par flotteurs. Houille Blanche (9), 242–248. http://dx.doi.org/10.1051/lhb/1910058.

Carufel, L.H., 1980. Construction and Use of a Velocity Head Rod for Measuring Mountain Stream Velocity and Flow. Technical Report 5, BLM/Alaska, p. 10.

Cohn, T., Kiang, J., Mason, R., 2013. Estimating discharge measurement uncertainty using the interpolated variance estimator. J. Hydraul. Eng. 139 (5), 502–510.

Costa, J.E., Cheng, R.T., Haeni, F.P., Melcher, N., Spicer, K.R., Hayes, E., Plant, W., Hayes, K., Teague, C., Barrick, D., 2006. Use of radar to monitor stream discharge by noncontact methods. Water Resour. Res. 42, 1–14.

Davids, J.C., Rutten, M.M., Pandey, A., Devkota, N., van Oyen, W.D., Prajapati, R., van de Giesen, N., 2019. Citizen science flow – an assessment of simple streamflow measurement methods. Hydrol. Earth Syst. Sci. 23 (2), 1045–1065.

Despax, A., Hauet, A., Le Coz, J., Dramais, G., Blanquart, B., Besson, D., Belleville, A., 2017. Inter-Laboratory Comparison of Discharge Measurements with Acoustic Doppler Current Profilers. Chauvan Field Experiments, 8, 9 and 10th November 2016. Preliminary Report. Technical report, Groupe Doppler Hydrométrie, p. 75.

Despax, A., Le Coz, J., Hauet, A., Mueller, D.S., Engel, F.L., Blanquart, B., Renard, B., Oberg, K.A., 2019. Decomposition of uncertainty sources in acoustic Doppler current profiler streamflow measurements using repeated measures experiments. Water Resour. Res. 55 (9), 7520–7540. http://dx.doi.org/10.1029/2019WR025296.

Despax, A., Le Coz, J., Mueller, D.S., Hauet, A., Calmel, B., Pierrefeu, G., Naudet, G., Blanquart, B., Pobanz, K., 2023. Validation of an uncertainty propagation method for moving-boat acoustic Doppler current profiler discharge measurements. Water Resour. Res. 59 (1), http://dx.doi.org/10.1029/2021WR031878.

Despax, A., Perret, C., Garçon, R., Hauet, A., Belleville, A., Le Coz, J., Favre, A.-C., 2016. Considering sampling strategy and cross-section complexity for estimating the uncertainty of discharge measurements using the velocity-area method. J. Hydrol. 533, 128–140.

Di Fidio, M., Gandolfi, C., 2011. Flow velocity measurement in italy between renaissance and risorgimento. J. Hydraul. Res. 49 (5), 578–585. http://dx.doi.org/10.1080/00221686.2011.594599.

Drost, H., 1963. Velocity-head rod for measuring stream flow. J. Hydrol. (New Zealand) 2, 7–11.

Fonstad, M.A., Reichling, J.P., Van de Grift, J.W., 2005. The transparent velocity-head rod for inexpensive and accurate measurement of stream velocities. J. Geosci. Educ. 53 (1), 44–52.

Fujita, I., Muste, M., Kruger, A., 1998. Large-scale particle image velocimetry for flow analysis in hydraulic engineering applications. J. Hydraul. Res. 36, 397–414.

Guglielmini, D., 1690. Aquarum fluentium mensura nova methodo inquisita (investigations on a new method of flowing water measurement) [in latin]. In: Typographia Pisariana, Bononiae.

Hauet, A., Morlot, T., Daubagnan, L., 2018. Velocity Profile and Depth-Averaged To Surface Velocity in Natural Streams: A Review over Alarge Sample of Rivers. Vol. 40, http://dx.doi.org/10.1051/e3sconf/20184006015.

Heede, B.H., 1974. Velocity-Head Rod and Current Meter Use in Boulder-Strewn Mountain Streams. Forest Service Research Note RM-271, USDA, p. 4.

Hilgersom, K.P., Luxemburg, W.M.J., 2012. Technical note: How image processing facilitates the rising bubble technique for discharge measurement. Hydrol. Earth Syst. Sci. 16, 345–356.

Hundt, S., Blasch, K., 2019. Laboratory assessment of alternative stream velocity measurement methods. PLoS One 14 (9).
ISO748:2009, 2009. Hydrometry - measurement of liquid flow in open channels using current-meters or floats.
ISO/TS25377:2007, 2009. Hydrometric uncertainty guidance (HUG).
JCGM 100:2008, 2008. Evaluation of Measurement Data – Guide To the Expression of Uncertainty in Measurement (GUM). Technical Report, JCGM Member Organizations (BIPM, IEC, IFCC, ILAC, ISO, IUPAC, IUPAP and OIML).
King, T., Hundt, S., Simonson, A., Blasch, K., 2022. Evaluation of select velocity measurement techniques for estimating discharge in small streams across the United States. J. Am. Water Resour. Assoc. 58 (6), 1510–1530.
Le Coz, J., Blanquart, B., Pobanz, K., Dramais, G., Pierrefeu, G., Hauet, A., Despax, A., 2016. Estimating the uncertainty of streamgauging techniques using in situ collaborative interlaboratory experiments. J. Hydraul. Eng. 142 (7), 04016011.
Le Coz, J., Camenen, B., Dramais, G., Ferry, M., Rosique, J.-L., Ribot-Bruno, J., 2011. Contrôle des débits réglementaires. Application de l'article L. 214-18 du code de l'environnement [inspection of statutory discharges. Application of the L. 21418 article of the environment code, in French].
Le Coz, J., Camenen, B., Peyrard, X., Dramais, G., 2012. Uncertainty in open-channel discharges measured with the velocity-area method. Flow Meas. Instrum. 26, 18–29.
Le Coz, J., Camenen, B., Peyrard, X., Dramais, G., 2015. Erratum - uncertainty in open-channel discharges measured with the velocity-area method. Flow Meas. Instrum. 46, 193–194.
Le Coz, J., Hauet, A., Pierrefeu, G., Dramais, G., Camenen, B., 2010. Performance of image-based velocimetry (LSPIV) applied to flash-flood discharge measurements in Mediterranean rivers. J. Hydrol. 394, 42–52.
Le Coz, J., Renard, B., Vansuyt, V., Jodeau, M., Hauet, A., 2021. Estimating the uncertainty of video-based flow velocity and discharge measurements due to the conversion of field to image coordinates. Hydrol. Process. 35 (5).
L'Hôte, Y., 1990. Historique du concept de cycle de l'eau et des premières mesures hydrologiques en Europe [History of the water cycle concept and of the first hydrological measurements in Europe, in French]. Hydrol. Contin. 5 (1), 13–27.
McMillan, H., Seibert, J., Petersen-Øverleir, A., Lang, M., White, P., Snelder, T., Rutherford, K., Krueger, T., Mason, R., Kiang, J., 2017. How uncertainty analysis of streamflow data can reduce costs and promote robust decisions in water management applications. Water Resour. Res. 53 (7), 5220–5228.
Muste, M., Fujita, I., Hauet, A., 2008. Large-scale particle image velocimetry for measurements in riverine environments. Water Resour. Res. 46 (4), http://dx.doi.org/10.1029/2008WR006950.
Pernot, F., 2018. Elaboration de Systèmes de Jaugeage à bas Coût [Development of low-cost Streamgauging Systems]. Technical report, Irstea / Polytech Nice-Sophia, p. 48.
Pike, R.G., Redding, T.E., Schwarz, C.J., 2016. Development and testing of a modified transparent velocity-head rod for stream discharge measurements. Can. Water Resour. J. 41 (3), 372–384.
Storz, S.M., 2016. Stage-Discharge Relationships for Two Nested Research Catchments of the High-Mountain Observatory in the Simen Mountains National Park in Ethiopia (Master's thesis). Bern University, Switzerland, p. 87.
Strobl, B., Etter, S., van Meerveld, I., Seibert, J., 2020. Accuracy of crowdsourced streamflow and stream level class estimates. Hydrol. Sci. J. 65 (5), 823–841.
Welber, M., Le Coz, J., Laronne, J., Zolezzi, G., Zamler, D., Dramais, G., Hauet, A., Salvaro, M., 2016. Field assessment of non-contact stream gauging using portable surface velocity radars (SVR). Water Resour. Res. 52, 1108–1126.
Wilding, T., Bulleid, J., Smith, B., Thyne, G., Elley, G., Starr, A., 2016. Better flow measurements in slow, weedy streams -using the Rising Bubble method. In: 2016 NZHS Technical Workshop, Gisborne, New Zealand.
Wilm, H.G., Storey, H.C., 1944. Velocity head rod calibrated for measuring streamflow. Civ. Eng. 14 (11), 475–476.